dynamics (North-Holland, Amsterdam, 1974), Chap. 5.

[8]Ref. 1 and also K. R. Atkins and I. Rudnick, in *Progress in Low Temperature Physics*, edited by C. J. Gorter (North-Holland, Amsterdam, 1970), Vol. 6.

[9]The epoxy beads used to maintain the capacitor gap could also couple the third sound on the two plates. Because of the small bead size and the large size of the bolometer signals, we are convinced that this is not the primary cause of the twin wave.

[10]R. K. Galkiewicz, K. L. Telschow, and R. B. Hallock, J. Low Temp. Phys. 26, 147 (1977).

[11]J. H. Scholtz, E. O. McLean, and I. Rudnick, Phys. Rev. Lett. 32, 147 (1974).

[12]K. R. Atkins, Phys. Rev. 113, 962 (1959).

Dynamical Calculations of Low-Energy Electron Diffraction for Incommensurate Lattice Structures—Xe on Ag(111)

N. Stoner,[a] M. A. Van Hove, and S. Y. Tong

Department of Physics and Surface Studies Laboratory, University of Wisconsin, Milwaukee, Wisconsin 53201

and

M. B. Webb

Department of Physics, University of Wisconsin, Madison, Wisconsin 53706

(Received 5 August 1977)

Dynamical calculations of low-energy-electron-diffraction intensity-voltage curves are carried out for the first time for the case of an incommensurate overlayer-substrate system, Xe-Ag(111). A new scheme was developed to take into account that the substrate (or overlayer) has incident upon it electron beams at angles unrelated to those angles into which the substrate (overlayer) itself diffracts beams. Comparing the calculated curves with experiment, a Xe-Ag(111) spacing of 3.55 ± 0.1 Å is determined.

Dynamical calculations of low-energy electron diffraction (LEED) has, in the past, succeeded in determining the surface structures of a number of metals, semiconductors, and ordered overlayer systems.[1,2] However, up to now, no successful dynamical calculation has been made on systems where an ordered overlayer is out of registry with the substrate lattice, i.e., the overlayer and substrate lattices are incommensurate with each other. A system of this kind of particular interest is the Xe monolayer on Ag(111).[3-5] The system involves the physisorption of a noble gas on a transition metal substrate. Many studies have been made on surface interaction forces of such systems,[6,7] but there is little detailed knowledge of atomic spacings at the surface.

Extensive LEED experimental data have been gathered on the Xe-Ag(111) system. Chesters, Hussain, and Pritchard[5] studied this system at liquid nitrogen temperatures. They established that the Xe monolayer forms a hcp lattice on the Ag(111) substrate. Webb and co-workers[3,4] recently made extensive measurements of intensity-voltage (I V) curves at 25 K. From the two-dimensional spot pattern, they determined that the Xe lattice is out of registry with the Ag substrate, requiring either a contraction of 2.8% or an expansion of 12.3% (plus a 30° rotation) to become integrally related to the substrate.[3]

An important structural parameter is the interlayer Xe-Ag distance, a distance determined by adsorbate-substrate interaction forces. From LEED, this distance can only be determined by analyzing intensity-voltage data.[1,2] We have carried out a dynamical calculation of IV curves for the Xe-Ag(111) system. Because the lattice is incommensurate, Xe atoms take a continuum of lateral positions relative to the Ag unit mesh and this causes a number of problems which require special treatment in the theoretical method. In a LEED calculation of integrally related overlayer-substrate systems, the beam set of the substrate is always a subset of that of the overlayer. Multiple scatterings between the overlayer and substrate simply redistribute electron amplitudes among a finite set of beams.[8] In the case of an incommensurate overlayer-substrate system, there are two entirely independent, unrelated beam sets. The fact that the overlayer beams, $\vec{g}$, are unrelated to the substrate beams, $\vec{G}$, [except, of course, for the (00) beam], implies that the substrate has incident on its surface beams at angles *unrelated* to those angles into which the substrate itself diffracts beams. The layer scattering matrices normally calculated in LEED theory[8] do not include the proper matrix elements

to describe this process. Therefore, a special scheme was used to locate and calculate the substrate matrix elements needed for the $\vec{k}_{in}+\vec{g}$ directions ($\vec{k}_{in}$ is the incident electron momentum). Similarly, the Xe overlayer experiences additional diffraction beams incident from the substrate in direction $\vec{k}_{in}+\vec{G}$. The same scheme was used to locate and calculate the necessary overlayer matrix elements to describe diffraction by the overlayer.

The overlayer and substrate constitute two separate scattering entities for which multiple scatterings within each can be solved independently. In the overlayer-substrate interface, an analytical perturbation procedure was used to sum and group scattering events (all backscatterings) in the order of relative magnitudes. In most cases, algebraic expressions can be obtained for the infinite-order sum of a given type of scattering event. For example, an event corresponding to multiple reflections in the incident (00) direction (summed to any order), followed by a substrate scattering into direction $\vec{k}_{in}+\vec{G}$, then multiple reflections in the $\vec{k}_{in}+\vec{G}$ direction (to any order), scattering back into the incident direction, and finally, multiple reflections in the incident direction (to any order), is evaluated by the algebraic formula

$$S=t_{\vec{0}\vec{0}}P_{\vec{0}}^{-}[1-R_{\vec{0}\vec{0}}P_{\vec{0}}^{+}r_{\vec{0}\vec{0}}P_{\vec{0}}^{-}]^{-1}[1-P_{\vec{G}}^{+}r_{\vec{0}\vec{0}}^{\vec{G}}P_{\vec{G}}^{-}R_{\vec{G}\vec{G}}]^{-1}$$
$$\times[R_{\vec{0}\vec{G}}P_{\vec{G}}^{+}r_{\vec{0}\vec{0}}^{\vec{G}}P_{\vec{G}}^{-}R_{\vec{G}\vec{0}}][1-P_{\vec{0}}^{+}r_{\vec{0}\vec{0}}P_{\vec{0}}^{-}R_{\vec{0}\vec{0}}]^{-1}P_{\vec{0}}^{+}t_{\vec{0}\vec{0}}. \quad (1)$$

In Eq. (1), the factors $P_{\vec{G}}^{\pm}$ represent + (inward) and − (outward) propagations in the direction $\vec{k}_{in}+\vec{G}$ in the interface region. Matrix elements $t_{\vec{g}\vec{g}}$, $r_{\vec{g}\vec{g}}^{\vec{G}}$, and $R_{\vec{G}\vec{G}}^{\vec{g}}$ denote transmission and reflection processes, t and r for the overlayer, R for the substrate. The subscripts on t, r, and R indicate electron amplitudes being diffracted from one beam to another. The superscripts are used to indicate the incoming beam direction. The groups of scattering events are summed and the final calculated intensity tested for numerical convergence.

Even with this procedure, there was a class of scattering events (the only group) that was excluded in our calculation. This class contains events such as starting in an incident direction $\vec{k}_{in}$, scattering by an overlayer beam into the $\vec{k}_{in}+\vec{g}$ direction, followed by a substrate scattering into $\vec{k}_{in}+\vec{g}+\vec{G}$, and so on. These overlayer-substrate beam mixing events lead to divergent number of beams in a multiple scattering formalism. Each higher-order event brings in more beam directions. Fortunately, we can establish later in this Letter that the lowest order (i.e., the largest value) of a beam mixing event that scatters into the $\vec{g}$ or $\vec{G}$ directions has magnitude *smaller* than the cutoff defined for good numerical convergence of the calculated *IV* curves. Thus, their exclusion in the calculation does not cause any numerical inaccuracy.

It should be pointed out that even with the exclusion of beam mixing events, the computation effort required for calculating *IV* curves of an incommensurate system is considerably greater than that of integrally related systems. For example, using 55 overlayer beams and 29 substrate beams, the calculation at a given electron incident direction is, in principle, comparable to separate computations at 84 different incident angles. Fortunately, with the use of beam symmetry,[8] algebraic perturbation formulas, and storing frequently used vectors and matrices, the total computation time was kept to manageable levels.

First, we wish to establish the accuracy of the computation. The electron scattering may be separated into three major categories: (i) electrons scattered into the (00) beam, (ii) electrons scattered into a Xe beam $\vec{g}$, and (iii) electrons scattered into a substrate beam $\vec{G}$. Diagrams representing scattering events that diffract electrons into the (00) beams are shown in Fig. 1(a). The dominant events are first-order (1 and 2) and third-order (3 and 4) nonzero-angle scatterings. Higher orders, including sums over infinite orders, are also included (events 5 to 7, and any combinations of them). The lowest-order beam mixing events are shown in 8 and 9. The (00) beam *IV* curve is shown in Fig. 2(a). The solid line is the result of including events up to third order. The calculated curve including fourth- and higher-order events is indistinguishable from the solid curve of Fig. 2(a). In other words, inclusion of events up to third order is numerically accurate for the (00) beam. All higher-order events are small and may be excluded. Since the lowest-order beam mixing events (Fig. 1, diagrams 8 and 9) are fourth order, they can be excluded. It should be pointed

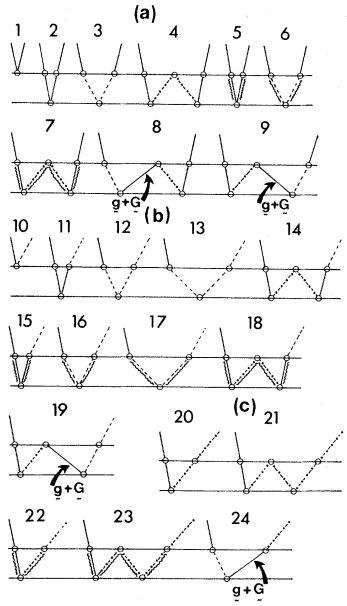

FIG. 1. Scattering events between overlayer and substrate. Broken line, $\vec{g}$ scattering; chain line, $\vec{G}$ scattering; wavy line, infinite order of an event; circle, exact overlayer (substrate) scattering.

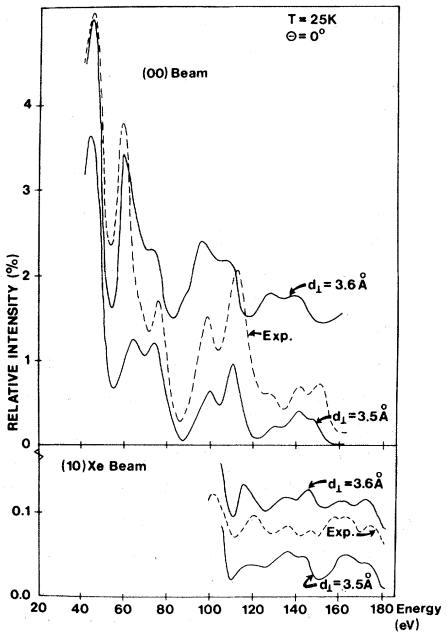

FIG. 3. Comparisons of calculated (00) and (10) Xe beams with experiment.

out that a first-order event does not mean *single* scattering. It actually includes many intralayer Xe scatterings and many interlayer and intralayer substrate scatterings.

For an overlayer beam, the different types of scattering events are shown in diagrams 10–19,

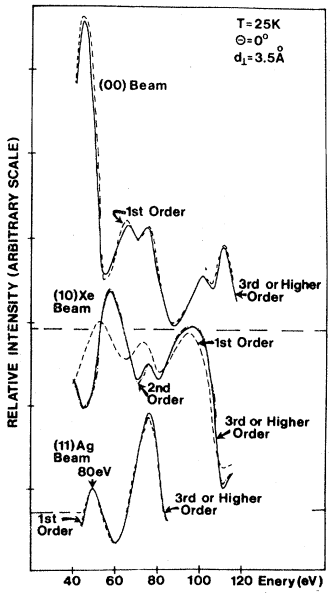

FIG. 2. Calculated *IV* curves for various orders. The (11) beam is shifted down by 30 eV.

Fig. 1(b). The corresponding calculated *IV* curve for the (10) Xe beam is shown in Fig. 2(b). In this case, we found that it is important to include up to second-order events [diagrams 10–12, Fig. 1(b)], producing the chain curve in Fig. 2(b). Higher-order scattering events (third and higher) produce negligible differences in the *IV* curve [solid line, Fig. 2(b)]. Our calculations include all diagrams (10–18) and any combinations of them, excluding only beam mixing events (19). Since the dominant contributions of beam mixing events to $\vec{g}$ or $\vec{G}$ directions are third and higher orders, their exclusion is numerically justified. Scattering events into a substrate beam are shown in diagrams 20–24, Fig. 1(c). From the calculated *IV* curve for the (11) substrate beam [Fig. 2(c)], it can again be established that beam mixing terms (third order and higher) may be excluded.

This theoretical procedure was used to calculate *IV* curves for different beams to extract the Xe-Ag(111) surface spacing by comparing with corresponding experimental data. Since the overlayer and substrate lattices are incommensurate, the resulting overlayer surface may not be exactly planar. The calculation assumes a planar Xe overlayer, hence the d spacing determined represents an effective interlayer distance. Calculations were made for a range of d spacings,

from 3.3 to 3.8 Å, in steps of 0.1 Å. The minimum d spacing corresponds to the case where a Xe atom sits in a bridge (twofold symmetry) site. A constant inner potential $V_0 = 10$ eV is used for both the overlayer and substrate. The calculated IV curves were compared with the data of Webb and co-workers.[3,4] Figure 3 shows the comparisons for the (00) and (10) beams. From the comparison, we conclude that the optimal spacing is between 3.5 and 3.6 Å. We put it at 3.55 ± 0.1 Å. This result compares favorably to the result 3.5 ± 0.1 Å reported by Webb and co-workers.[3,4] Their result was obtained by data averaging over many incident angles.

It is apparent that the dynamical LEED approach may be appropriately modified to analyze surface structures of irrationally related lattices. It is probably due to the weak scattering power of Xe that we can completely neglect beam mixing terms in this work; however, because the theoretical method includes many more scattering events (third and higher orders for many events), we believe this procedure, with minor modifications, can adequately treat many of the stronger overlayer scatterers that are irrationally related to the substrate. In fact the importance of the beam mixing events can be estimated directly by inspection of the data prior to any calculation. The small peak at $\vec{g} + \vec{G}$ labeled "multiple scattering" in Fig. 4 of Ref. 4 results from such an event and such contributions to specular, overlayer, and substrate beams must be smaller than this peak by at least one order.

We would like to thank Dr. P. I. Cohen for helpful discussions in the beginning stages of this work. This work was partially supported by a state of Wisconsin research grant, and also in part by National Science Foundation Grants No. DMR73-02614 and No. DMR74-1197.

[a]Also at Department of Physics, University of Wisconsin-Whitewater, Whitewater, Wisc.

[1]P. M. Marcus, *Characterization of Metal and Polymer Surfaces* (Academic, New York, 1977), Vol. 1, p. 271.

[2]P. M. Estrup and E. G. McRae, Surf. Sci. 25, 1 (1971).

[3]M. B. Webb and P. I. Cohen, CRC Solid State Sci. 6, 253 (1976).

[4]P. I. Cohen, J. Unguns, and M. B. Webb, Surf. Sci. 58, 429 (1976).

[5]M. A. Chesters, M. Hussain, and J. Pritchard, Surf. Sci. 35, 161 (1973).

[6]G. G. Kleiman and U. Landman, Phys. Rev. Lett. 31, 707 (1973), and Phys. Rev. B 12, 5484 (1973).

[7]J. P. Hobson, CRC Solid State Sci. 4, 221 (1974).

[8]N. Stoner, M. A. Van Hove, and S. Y. Tong, *Characterization of Metal and Polymer Surfaces* (Academic, New York, 1977), Vol. 1, p. 299.

Preparation of Literally Two-Dimensional Magnets

M. Pomerantz, F. H. Dacol, and Armin Segmüller
IBM Thomas J. Watson Research Center, Yorktown Heights, New York 10598
(Received 9 September 1977)

The Langmuir-Blodgett technique was used to deposit manganese stearate in the form of monolayers. Because of the nature of the method, and a variety of supporting experiments, it is concluded that the Mn atoms are arrayed on a single surface, thus forming literally two-dimensional magnetic materials.

There has been a great amount of theory of model magnetic systems in two spatial dimensions.[1] Experimental work to test the theories has also been extensive in recent years.[2] The experiments have, with one exception,[3] been done on materials that were three-dimensional, layer-like structures, and hence were "quasi two-dimensional." In these experiments the question remains of the influence of the third dimension. In this Letter we outline the preparation and characterization of *literally* two-dimensional (2-D) magnetic structures. Evidence for magnetic ordering at low temperatures will be published elsewhere.

We achieve exact two-dimensionality by depositing the magnetic materials in individual sheets that are one molecule thick. The method we used was an application of the well-known Langmuir-Blodgett technique.[4] Briefly, stearic acid, a long-chain fatty acid with formula $HOOC\text{-}(CH_2)_{16}\text{-}CH_3$, was spread on the surface of the water. The acidic "heads," $HOOC\cdots$, of these molecules tend to dissolve in water, releasing H^+; the fatty "tails," $(CH_2)_{16}\text{-}CH_3$, tend to float on the water